European Review for Medical and Pharmacological Sciences 2023; 27: 7793-7810

Functional assessment in endometrial and cervical cancer: diffusion and perfusion, two captivating tools for radiologists

F. DE MUZIO[1], R. FUSCO[2], I. SIMONETTI[3], F. GRASSI[4,5], R. GRASSI[4,5], M.C. BRUNESE[6], L. RAVO[7], N. MAGGIALETTI[8], R. D'ANIELLO[9], F. GRECO[10], M. GABELLONI[11], V. GRANATA[3]

[1]Department of Medicine and Health Sciences "V. Tiberio", University of Molise, Campobasso, Italy
[2]Medical Oncology Division, Igea SpA, Naples, Italy
[3]Division of Radiology, "Istituto Nazionale Tumori IRCCS Fondazione Pascale – IRCCS di Napoli", Naples, Italy
[4]Division of Radiology, "Università degli Studi della Campania Luigi Vanvitelli", Naples, Italy
[5]Italian Society of Medical and Interventional Radiology (SIRM), SIRM Foundation, Milan, Italy
[6]Department of Medical and Surgical Sciences & Neurosciences, Diagnostic Imaging Section, University of Molise, Campobasso, Italy
[7]Division of Radiology, Università degli Studi di Napoli Federico II, Naples, Italy
[8]Department of Medical Science, Neuroscience and Sensory Organs (DSMBNOS), University of Bari "Aldo Moro", Bari, Italy
[9]Hospital Pharmacy Division, Istituto Nazionale Tumori IRCCS Fondazione Pascale-IRCCS di Napoli, Naples, Italy
[10]Department of Medicine and Health Sciences "V. Tiberio", University of Molise, Campobasso, Italy
[11]Department of Translational Research and of New Surgical and Medical Technology, Academic Radiology, University of Pisa, Pisa, Italy

Abstract. **Uterine cervical and endometrial cancers are two major gynecological malignancies, affecting women's health worldwide.**

Magnetic resonance imaging (MRI) is appropriate for evaluating malignant disease, thanks to the excellent soft tissue contrast and multiplanar imaging ability. Recently, functional MR techniques, namely diffusion-weighted imaging (DWI) and dynamic contrast-enhanced imaging (DCE), have proved to be a precious support not only in cancer diagnosis but also in disease staging, in the therapy planning, in monitoring response to treatment and during long-term recurrence surveillance.

In the field of gynecologic oncology, the European Society of Urogenital Radiology (ESUR) recommends DWI and dynamic contrast-enhanced imaging (DCE-MRI) for local staging of endometrial and cervical cancer, but the potential application of functional imaging in all different aspects of patient management seems very promising.

The aim of this article is to summarize the existing literature, providing a comprehensive update on the role of functional MRI in endometrial and cervical cancer.

Key Words:
Endometrial Cancer, Cervical Cancer, DWI, IVIM, DKI, DCE-MRI.

Introduction

Uterine cervical and endometrial cancers (EC) are two major gynecological malignancies, affecting women's health worldwide[1]. In line with the International Federation of Gynecology and Obstetrics (FIGO) recommendations, the European Society of Urogenital Radiology (ESUR) recognizes the crucial role of imaging in EC and cervical cancer (CC), especially magnetic resonance imaging (MRI)[2]. MRI is appropriate for evaluating malignant disease, thanks to the excellent soft tissue contrast and multiplanar imaging ability[3-6]. Recently, functional MR techniques, namely diffusion-weighted imaging (DWI) and dynamic contrast-enhanced imaging (DCE-MRI), have proved to be a precious support not only in cancer diagnosis but also in disease staging, in therapy planning, in monitoring response to treatment and during long-term recurrence surveillance[7].

DWI enables the noninvasive characterization of biological tissues based on their water diffusion properties, which could be quantified by the apparent diffusion coefficient (ADC)[8-10]. In addi-

Corresponding Author: Roberta Fusco, MD; e-mail: r.fusco@igeamedical.com

tion to the classically applied single-exponential model, new mathematical models, such as Intravoxel Incoherent Motion (IVIM) and Diffusion Kurtosis Imaging (DKI), have been introduced in the field of oncology[11-13]. IVIM is a bi-exponential model that could separate the pure tissue diffusion aspect described by the D coefficient from microcapillary perfusion through the calculation of pseudo-diffusion coefficient (D*), and perfusion fraction (f)[11-13]; DKI could represent more faithfully the non-Gaussian movement of water molecules *in vivo*, providing two parameters: the kurtosis median coefficient (MK), which assesses the deviation of the tissue diffusion from the Gaussian model, and the diffusion coefficient (MD), which expresses the correction of the non-Gaussian bias[14].

DCE-MRI evaluates tissue perfusion by acquiring multiple sequential T1-weighted (T1W) images, after contrasting medium administration[15,16]. The perfusion examination presents different degrees of complexity and varies from a purely qualitative assessment of the time-intensity curves (TIC) to the application of an analysis based on pharmacokinetic models (Tofts Model and Brix model) that measure for each voxel the transfer rate of contrast agent[17,18].

In the field of gynecologic oncology, the ESUR panel recommends DWI and DCE-MRI for local staging of EC and CC, but the potential application of functional imaging in all different aspects of patient management seems very promising[19].

The aim of this article is to summarize the existing literature, providing a comprehensive update on the role of functional MRI in EC and CC.

Endometrial Cancer

Endometrial cancer is the seventh most common cancer in women, with an overall incidence of 417,367 cases and 97,370 deaths in 2020[20]. Most cases occur in post-menopausal women between the ages of 65 and 75, related to prolonged exposure to unopposed estrogen (nulliparity, estrogen-producing tumors, polycystic ovarian syndrome (PCOS), hormone replacement, and tamoxifen therapy) and metabolic conditions such as obesity and diabetes[20]. In addition to sporadic forms, which comprise around 90% of carcinomas, 10% are linked to hereditary syndromes such as hereditary non-polyposis colorectal cancer (HNPCC) and Lynch syndrome[20].

Endometrial tumors arise from Mullerian-derived glandular cells. In 1983, Bokhman[21], on the basis of a prospective clinic-pathological study, formulated the hypothesis of the existence of two variants of EC with different pathogenesis: 1) endometrioid carcinoma type I, estrogen-dependent, which are well-moderately differentiated carcinomas; 2) non-endometrioid carcinoma type II, non-estrogen-dependent, including poorly differentiated lesions with more rapid and unfavorable clinical evolution[22,23].

EC is surgically staged using the FIGO system[24]. The standard surgical procedure includes hysterectomy, bilateral salpingo-oophorectomy, lymph node dissection, peritoneal washing, and omental biopsies[24]. Although FIGO stage correlates with prognosis, preoperative assessment is essential to stratify patients according to risk and establish the possibility of less destructive interventions in selected categories[20,24]. In particular, it is crucial to identify in childbearing age patients with grade 1 endometrioid adenocarcinoma those with endometrium-confined disease, who could benefit from fertility-sparing treatment[20,24]. Moreover, current evidence[25] suggests that lymphadenectomy may be avoided in patients with low-risk features on imaging, including less than 50% myometrial invasion, tumor lesion diameter <2 cm, and well- or moderately differentiated histology. Indiscriminative lymphadenectomy may lead to overtreatment and increase post-operative complications that may negatively impact the quality of life[26,27].

The major factors related to the prognosis of EC comprise tumor grade and subtype, depth of myometrial invasion (Figure 1), cervical stromal infiltration (CSI), lymphovascular space invasion (LVSI), and nodal status[28]. Functional MRI has been demonstrated to provide biomarkers of several prognostic factors, helping in the establishment of a personalized therapeutic approach[28,29].

DWI

DWI showed an association between the ADC of the primary tumor and the disease extent[30,31]. Furthermore, an inverse relationship between ADC and pathologic grade has been consistently reported[30-33]. Specifically, Reyes-Pérez et al[34] observed that the mean ADC values (ADCmean) and minimum ADC (ADCmin) values were significantly lower for patients with G2 and G3 endometrial tumors than for those with G1 lesions, in a sample of 48 pathologically confirmed cases of EC, reviewed

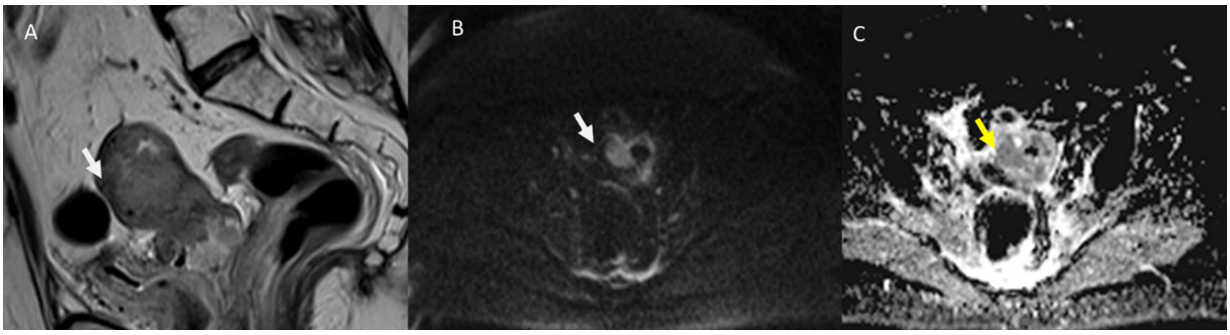

Figure 1. MRI (1.5 T Magnetom Symphony scanner (Siemens AG, Erlangen, Germany), equipped with an 8-element body and phased array coils) assessment of EC (arrow) with myometrial and cervical involvement. **A**, (Turbo spin echo (TSE) T2-W in the sagittal plane) the lesion shows hyperintense signal with restricted signal in DWI [(**B**) b 800 s/mm^2) and hypointense signal in ADC map (**C**). The figure was obtained by images from the Division of Radiology, "Istituto Nazionale Tumori IRCCS Fondazione Pascale – IRCCS di Napoli", Naples, Italy.

retrospectively. These data are confirmed by a subsequent study by Ozturk et al[35] in a cohort of 83 patients, of which 60 with endometroid carcinoma and 23 with tumors of other subtypes. Among the endometroid-type, high-grade carcinomas showed reduced ADC values compared to low-grade ones[35]. Furthermore, ADCmean and ADCmin significantly differ between endometrioid and non-endometrioid lesions ($0.72/0.58\times10^{-3}$ mm^2/s and $0.82/0.63\times10^{-3}$ mm^2/s, respectively)[35]. This implied that the ADCmean and ADCmin values may be effective in diagnosing the most undifferentiated cancerous lesions. Both studies[34,35] were conducted on 3T scanners[34,35], but the same conclusions were also reached by Chen et al[36], using a 1.5 T scanner. However, these inferences would not seem to be generalizable, so simplistically. Indeed, Yan et al[33] observed that squamous differentiation may decrease ADCmean and ADCmin values of the endometroid subtype, while carcinosarcomas showed relatively high ADCmean values than other high-grade carcinomas.

Despite these limitations, ADC would appear to be a good surrogate in assessing tumor histological type and, thus, a useful element in risk stratification.

It should also be considered that in a not insignificant percentage of cases, there is a discrepancy between the tumor grade detected postoperatively and preoperatively[37]. Helpman et al[37] found a reclassification on the final surgical specimen of 22% of patients into G2-G3 or non-endometrioid tumors, in a cohort of 255 patients diagnosed as G1 endometrioid adenocarcinoma on biopsy. So, the ability to predict high-grade EC on MRI is of great interest, deserving further investigation.

Deep myometrial invasion (DMI) is an independent prognostic factor for lymph node metastasis (Figure 2). In some postmenopausal individuals or patients with a widened uterine cavity, identification of the junctional zone (JZ) could be difficult, leading to an inaccurate assessment of tumor extension[38]. The simultaneous presence of areas of adenomyosis or the location of the lesion

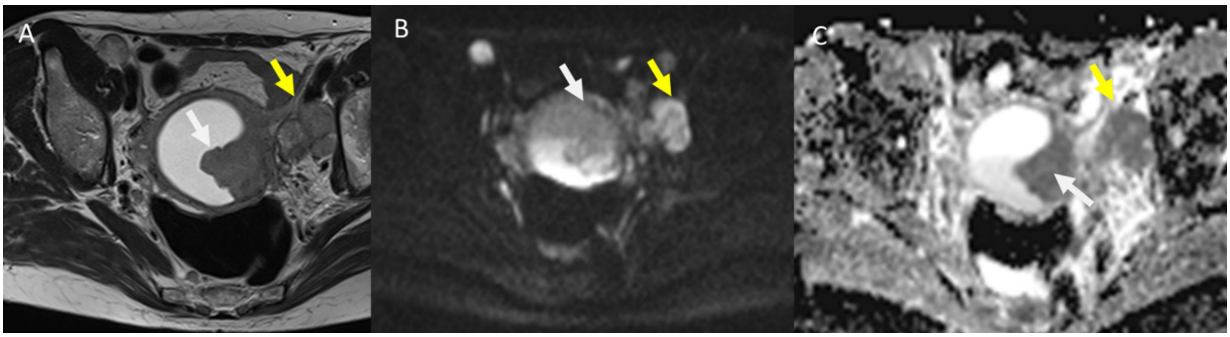

Figure 2. MRI (1.5T Magnetom Symphony scanner (Siemens AG, Erlangen, Germany), equipped with an 8-element body and phased array coils) assessment of EC (white arrows) with myometrial and nodal involvement (yellow arrows). **A**, (TSE T2-W in the axial plane), the lesion and nodes show hyperintense signal with restricted signal in DWI (**B**, b 800 s/mm^2) and hypointense signal in ADC map (**C**). The figure was obtained by images from the Division of Radiology, "Istituto Nazionale Tumori IRCCS Fondazione Pascale – IRCCS di Napoli", Naples, Italy.

in uterine cornua, physiologically thinner than the normal myometrium, may also increase the probability of staging misinterpretations[38]. DWI could define small endometrial lesions that may not be clearly visible on T2 weighted (T2W) image[39]. As reported by Song et al[39] in a prospective study, DWI not only recorded a higher sensitivity compared to T2W in identifying endometrial lesions (97% *vs.* 85%), but displayed an ability to enhance T2W in detection of small lesions (0.7-1 cm in diameter), that had been missed on first evaluation with the morphological sequence alone.

Recently, an attractive technical advancement named reduced field-of-view (rFOV) DWI has been introduced[40]. rFOV DWI yielded less distortion, improving image quality that could better outline anatomic details, entailing more accurate ADC measurements than full FOV-DWI[40]. Although rFOV proved to refine diagnostic performance for DMI in EC, it would appear to be incapable of increasing the diagnostic ability of MRI to reliably distinguish superficial myometrial invasion[40].

Another study technique that could potentially overcome these limitations is the fusion of morphological and functional sequences. Guo et al[41], in 58 ECs retrospectively enrolled, recorded higher diagnostic accuracy of T2W-DWI fusion respect to T2W alone to assess myometrial invasion (77.6% for T2W; 94.8% for T2W-DWI), distinguishing properly superficial from deep involvement.

There is much evidence suggesting that T2W can benefit of the contribution of both DWI and DCE sequences (Figure 3) for DMI. Andreano et al[42] reported no significant difference in the sensitivity or specificity between DWI and DCE-MR for diagnosing DMI. A large meta-analysis by Deng et al[43] confirmed similar diagnostic performance of DWI and DCE-MRI.

In the era of abbreviated MRI protocols and optimized medicine[44], short unenhanced protocols for EC staging have been proposed[45]. Thus, it is reasonable to consider acquiring DCE only in case of inconclusive agreement between the T2W and DWI[44,46,47].

Evolution of DWI Technique

ADC may reflect simultaneously restricted diffusivity and microperfusion phenomena, potentially leading to overlap between ADC values of different tumor grades[13,14]. The use of advanced diffusion models may lead to a more reliable preoperative prediction of tumor grade in EC. Chryssou et al[48] in prospective study included 52 women with EC, applying IVIM model to histogram analysis technique, recorded a lower interquartile range (IQR) of coefficient D in G1-G2 tumors compared to that of the G3 group. IQR D describes the distribution of pure water movement heterogeneity inside a lesion, while the mean D value reflects the average water diffusivity of all voxels[48]; different IQR D values between different grading groups may be explained by a more heterogeneous nature of the high-grade tumors[48,49]. So, IVIM model's parameter D, the true diffusion coefficient, seems to be able to differentiate between low- and high-grade lesions.

For purposes of confirming that the water diffusion distribution featured with non-Gaussian distribution in EC may be a more promising method of tumor grading than Gaussian distribution preoperatively, Chen et al[50] evaluated the utility of hi-

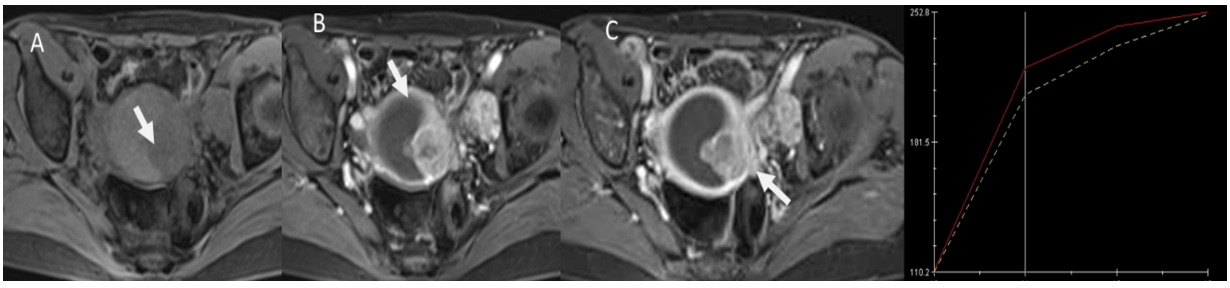

Figure 3. The same patient of Figure 2. DCE-MRI (1.5 T Magnetom Symphony scanner (Siemens AG, Erlangen, Germany), equipped with an 8-element body and phased array coils) assessment of EC with myometrial (white arrows) involvement. During dynamic evaluation [(**A**) T1W Volumetric interpolated breath-hold examination (VIBE) fat-saturated (FS) without contrast medium; (**B**) T1-W VIBE FS in arterial phase; (**C**) T1W VIBE FS during late phase (DCE-MRI)] the lesion shows progressive contrast enhancement with type II TIC (time-intensity curves). We employed the Gd-BT-DO3A (Gadovist, Bayer Schering Pharma AG, Berlin, German). The patient received 0.1 ml/kg of Gd-BT-DO3A by means of a power injector (Spectris Solaris® EP MR, MEDRAD Inc., Indianola, IA, USA), at an infusion rate of 2 ml/s. The figure was obtained by images from the Division of Radiology, "Istituto Nazionale Tumori IRCCS Fondazione Pascale – IRCCS di Napoli", Naples, Italy.

stogram analysis of DKI based on entire tumor volume in 73 patients. They demonstrated that DKI features resulted superior to other parameters in distinguishing high-grade from low-grade cancers [50].

Moreover, Yue et al[51] compared the performances of DKI and DWI for diagnosing and histologically grading EC. The MK values had the highest diagnostic accuracy in differentiating G0 and (G1+G2+G3), G0 and G1, G1 and G2, and G2 and G3 (AUC=0.93, 0.76, 0.91, 0.91, p-value <0.05). MK was maximally correlated with histological grade[51].

The depth of the myometrial invasion is strongly connected to the existence of lymph node metastasis and overall patient survival rate[52]. Specifically, the risk of lymph node involvement varies from 3%[53] to 46 % in case of superficial or deep invasion, respectively[54]. As previously mentioned, the predictive value of DWI alone on the degree of intramural tumor extension could be inadequate. This could be related to the method of region of interest delineation, or the mean ADC value used. Song et al[55] post-processed data from 118 pathologically confirmed EC patients with preoperative DWI, with a DKI (b value of 0, 700, 1,400, and 2,000 s/mm^2) model for quantitation of MD and MK for non-Gaussian distribution. A whole-tumor analysis approach was used, comparing the histogram parameters of D, K, and ADC for the DMI and superficial myometrial invasion subgroups. D10th showed a relatively higher AUC than ADC10th for the differentiation of lesions with DMI from those with superficial myometrial invasion (0.72 *vs.* 0.71), but the variation was not statistically significant (p-value = 0.35); both DKI and DWI models showed relatively equivalent effectiveness[55].

It would be crucial to assess simultaneous major prognosis risk factors related to patients' outcomes. Thus, the purpose of Zhang et al[28] was to quantitatively compare different models (mono-exponential, bi-exponential, and the stretched-exponential model proposed by Bennett et al[56]), aiming to intercept imaging markers that could facilitate the pre-treatment selection. Authors[28] measured and compared, in 61 samples of EC, histological grade, depth of myometrial invasion, CSI, and LVSI, confirmed by pathology. The combined parameters had more significant potential for evaluation of all risk factors assessed through multivariate logistic regression and the ROC curves, demonstrating the advantages of multiparametric MRI in pre-treatment choice of the optimal therapeutic approach[28].

This promising evidence advises that in the future, multiple DWI models could be used to evaluate EC, searching for a strategy to optimize the acquisition protocol by shortening the scan time and preserving the image quality.

DCE

DCE could be applied as a problem-solving tool when assessing the degree of myometrial invasion (Figure 4) and cervical stroma involvement in EC.

The JZ was found to be a notable landmark in defining the depth of myometrial invasion. The presence of a continuous low-signal-intensity JZ at T2W imaging could exclude myometrial infiltration[2]. As pointed out above, clinical conditions involving an alteration of the normal uterine anatomy could make evaluation quite complex[2,57]. DCE-MRI is a better tool compared to T2W in cases of a thickened or ill-defined JZ, as it enables a clear

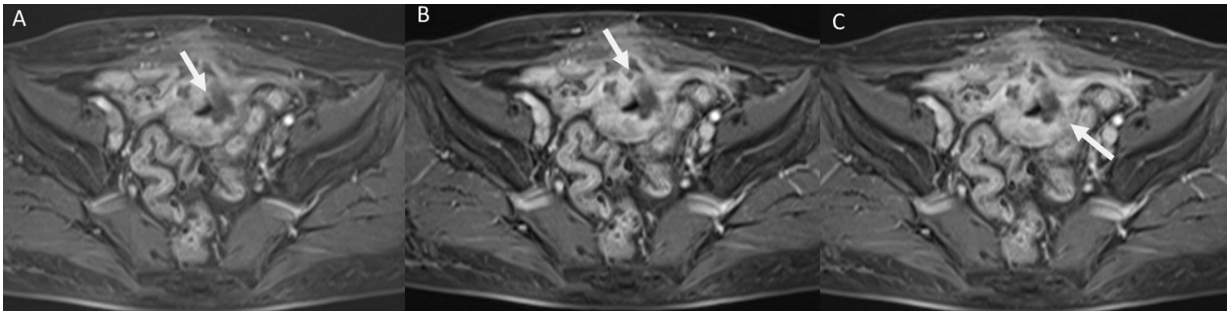

Figure 4. DCE-MRI (1.5T Magnetom Symphony scanner (Siemens AG, Erlangen, Germany), equipped with an 8-element body and phased array coils) assessment of EC with myometrial (white arrows) involvement. During dynamic evaluation, [(**A**), T1W VIBE FS without contrast medium; (**B**), T1W VIBE FS in the arterial phase (45 sec); (**C**), T1-W Vibe FS during late phase (120 sec)] the lesion shows progressive contrast enhancement. We employed the Gd-BT-DO3A (Gadovist, Bayer Schering Pharma AG, Berlin, German). The patient received 0.1 ml/kg of Gd-BT-DO3A by means of a power injector (Spectris Solaris® EP MR, MEDRAD Inc., Indianola, IA, USA), at an infusion rate of 2 ml/s. The figure was obtained by images from the Division of Radiology, "Istituto Nazionale Tumori IRCCS Fondazione Pascale – IRCCS di Napoli", Naples, Italy.

differentiation between the tumor and uterine wall layers[2]. Moreover, combining DCE-MRI and T2W led to a significant improvement in the diagnostic performance of MRI in all clinical scenarios[58]. A recent study showed that the diagnostic accuracy in detecting the depth of myometrial invasion of DCE and T2W is 78.12% and 75%, respectively, which could be significantly improved with the combination of DCE-MRI and T2W (90.62%)[58].

Considering the substantially overlapping diagnostic accuracy values between DCE and DWI, the use of contrast medium injection is controversial[38]. Furthermore, in view of an optimized protocol, the ESUR panel discussed the value of single-phase high spatial resolution contrast-enhanced imaging at 2 min 30 sec [the best time to depict microvascular invasion (MI)] *vs.* DCE-MRI[38]. Instead, DCE-MRI could be employed only in patients of childbearing age who desire fertility preservation and have grade 1 EC to confirm the endometrium-confined disease, which is best seen approximately 35-40 s following contrast injection[38]. This information could exclude any MI, confirming patient eligibility for conservative management[38].

MRI is the optimal imaging technique for preoperatively assessing cervical invasion[59]. In suspected cervical stroma involvement, accurate evaluation may guide the choice of a fertility-sparing approach or an adequate pathological tissue sampling[59]. On T2W, the cervical invasion occurs when abnormal intermediate to hyperintense mass is detected, causing a widening of the internal and cervical canal stroma in superficial mucosal involvement or when a direct disruption of the normal cervical stroma is recognized in deep cervical extent[59]. However, cervical stroma atrophy in postmenopausal women or large endometrial lesions could be a source of staging errors[60]. Freeman et al[60] reported an adjuvant value of DCE in distinguishing between stromal invasion and polypoid lesion protruding into the endocervix, reducing the false-positive rate of T2W[59]. Moreover, a recent meta-analysis[61] showed that DCE-MRI combined with T2W significantly improved the pooled specificity in stromal invasion detection, compared to T2W alone (95-100% and 86-95%, respectively).

During DCE study, irregular areas of interruption within normal enhanced epithelium could suggest cervical invasion[2]. Especially in the setting of T2W pitfalls, DCE could be an important instrument; in particular, delayed DCE-MRI (4-5 min after the injection) would seem to be the most informative on cervical involvement, as reported by the ESUR experts panel[2,59].

In Table I are reported the relevant functional studies in endometrial cancers.

Table I. Functional studies in endometrial cancers.

Authors	Tumor	Functional Assessment	Results
Yan et al[33]	Endometrial	Conventional DWI	Squamous differentiation may decrease ADCmean and ADCmin values of endometroid subtype, while carcinosarcomas showed relatively high ADCmean value than other high-grade carcinomas
Perez et al[34]	Endometrial	Conventional DWI	ADCmean and ADCmin values were significantly lower for patients with G2 and G3 endometrial tumors than for those with G1 lesions
Ozturk et al[35]	Endometrial	Conventional DWI	ADCmean and ADCmin significantly differ between endometrioid and non-endometrioid lesions
Song et al[39]	Endometrial	Conventional DWI	Higher sensitivity compared to T2W in identifying endometrial lesions (97% *vs.* 85%)
Chryssou et al[48]	Endometrial	IVIM	The true diffusion coefficient, seems to be able to differentiate between low- and high-grade lesions
Chen et al[50]	Endometrial	DKI	The 10th percentile AUC MD, MK's 90th percentile, and 10th percentile of ADC resulted superior to other parameters in distinguishing high-grade from low-grade cancers
Yue et al[51]	Endometrial	DKI	MK values had the highest diagnostic accuracy in differentiating histological grading
Freeman et al[60]	Endometrial	DCE-MRI	Adjuvant value in distinguishing between stromal invasion and polypoid lesion

ADC: Apparent Diffusion coefficient; ADCmean: mean value of Apparent Diffusion coefficient; ADCmin: minimum value of Apparent Diffusion coefficient; AUC: area under curve; MD mean diffusivity; MK mean of Kurtosis.

Cervical Cancer

Cervical cancer is the fourth most common cancer in women globally[62], with an estimated incidence of 604,127 cases and 341,831 deaths in 2020[1]. The main etiopathogenetic factor is persistent papillomavirus (HPV) infection, particularly the oncogenic subtypes (HPV 16 and 18)[63]. Despite screening programs with the Papanicolaou smear and early treatment of pre-cancerous lesions, CC is still a major public health problem even in developed countries, with more than 58,000 new cases diagnosed and approximately 24,000 patients dying in Europe each year[63].

In the recent past, the staging of CC was exclusively clinical, but given the documented inaccuracies, radical changes in management have been made. Under the 2018 FIGO guideline upgrade[64], imaging is formally incorporated as an indispensable supplement to clinical examination (i.e., pelvic examination, cystoscopy, and colposcopy) to obtain an accurate description of tumor spread[65]. The challenge at the diagnostic stage is to make the right decision during the multidisciplinary tumor board between surgery and chemoradiation therapy[64,65]. Over-staging could result in an aggressive surgical approach in women of childbearing age who may attempt fertility-preserving surgery; on the other hand, an underestimation of tumor spread may result in therapy failure with disease progression[64,65]. The elements to consider that may compromise the possibility of a surgical approach are a tumor mass greater than 4 cm, the invasion of parameters (Figure 5), the presence of lymph node metastases (Figure 6) or the extension of disease to adjacent organs (Figure 7).

Histological subtype and grade of differentiation may also influence the course of the disease, the therapeutic outcome and patient survival[66-68].

MRI is routinely employed for evaluating the local extent of CC, and DWI and DCE are already part of the standard MR work-up for CC assessment, as they allow information of the tumor microenvironment rather than pure conventional anatomical measurements[69,70].

DWI

On T2W, CC appears as a mass of intermediate/high signal, that stands out against a background of hypointense cervical stroma. However, there are conditions in which the precise definition of the lesion could be difficult to delineate, such as young patients with a less hypointense stroma and in the presence of pressure-induced changes or edema of peritumoral tissue[69]. DWI bears the potential to overcome these limits.

As with other malignant lesions, CC shows a hyperintense signal in DWI and lower ADC value compared to normal cervical tissue, due to the higher cell density[19,71]; this behavior could enable a precise demarcation of the tumor margins, providing excellent tumor-to-normal-tissue contrast[72,73]. A further improvement in tumor detection could be achieved by the application of a reduced FOV, with a significant refinement of image quality, as already seen in other gynecological malignancies[74,75].

Assessment of lymph vascular invasion and determination of lymph node metastases is also of primary importance in CC[69]. Both appear to be risk factors for disease recurrence (DR), affecting overall survival (OS)[19,69]. In oncological imaging, an involved lymph node is assumed to be increased in diameter, have a round contour, or have lost their fatty hilum[76-78]. On DWI, metastatic lymph nodes, generally may show a higher degree of re-

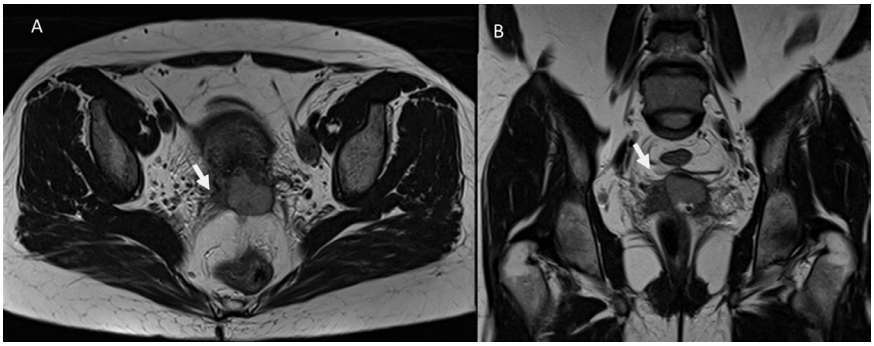

Figure 5. Conventional MRI (1.5 T Magnetom Symphony scanner (Siemens AG, Erlangen, Germany), equipped with an 8-element body and phased array coils). **A**, SE T2-W in the axial plane and (**B**) TSE T2-W in the coronal plane assessment of CC without stromal (white arrows) involvement. The lesion shows a hyperintense signal. The image was obtained by images from the Division of Radiology, "Istituto Nazionale Tumori IRCCS Fondazione Pascale – IRCCS di Napoli", Naples, Italy.

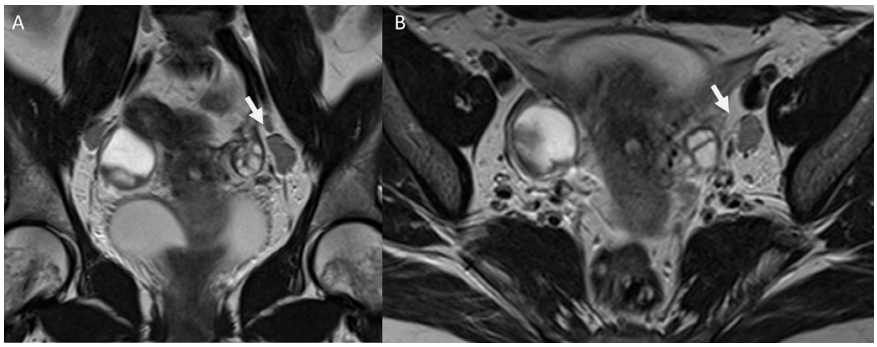

Figure 6. Conventional MRI [1.5 T Magnetom Symphony scanner (Siemens AG, Erlangen, Germany), equipped with an 8-element body and phased array coils). **A**, TSE T2-W in the coronal plane and (**B**) TSE T2-W in the axial plane] assessment of CC with node (white arrows) involvement. The node shows a hyperintense signal. The figure was obtained by images from the Division of Radiology, "Istituto Nazionale Tumori IRCCS Fondazione Pascale – IRCCS di Napoli", Naples, Italy.

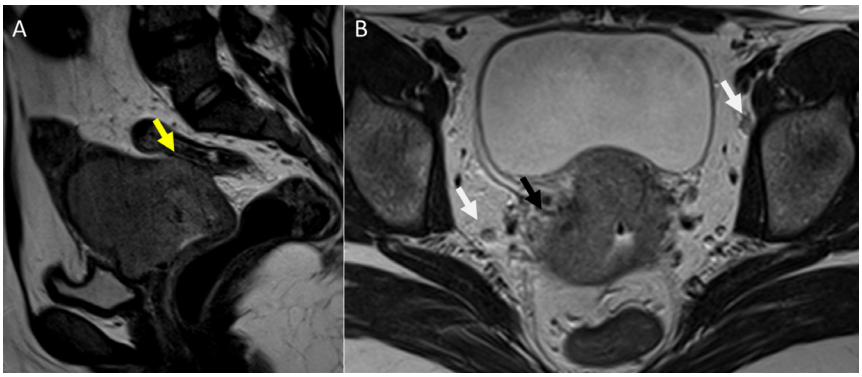

Figure 7. Conventional MRI (1.5 T Magnetom Symphony scanner (Siemens AG, Erlangen, Germany), equipped with an 8-element body and phased array coils). **A**, TSE T2-W in the sagittal plane and (**B**) TSE T2-W in the axial plane assessment of CC with rectal [white arrows in (**A**)], cervical stromal [black arrow in (B)] and nodes [white arrows in (**B**)] involvement. The figure was obtained by images from the Division of Radiology, "Istituto Nazionale Tumori IRCCS Fondazione Pascale – IRCCS di Napoli", Naples, Italy.

striction (Figure 8), which can be assessed quantitatively, using ADC values[76-78]. Using ADC values and lymph node size together showed increased sensitivity from 25% to 85% while keeping specificity relatively unchanged at 98-99%[77,78].

DWI also has a role in the assessment of parametrial involvement (Figure 9), as highlighted by reports on pathological proven parametrial invasion (PMI)[79,80]. Park et al[79] observed lower ADC values of cervical lesions in patients with pathologic PMI (0.874×10^{-3} mm^2/s), than those without parametrial involvement (0.995×10^{-3} mm^2/s), which was consistent with Nakamura et al[80] previous results (0.872 and 0.961×10^{-3} mm^2/s, respectively). This evidence reflected a diagnostic accuracy of 90% of DWI *vs.* 80% to 85% of T2W in the evaluation of PMI[79,80], further increased by fusion imaging application[81]. Mongula et al[81], in a prospective cohort of 65 patients planned for radical hysterectomy with pelvic lymphadenectomy (FIGO IA-IIA), documented a significant difference of positive predictive value between T2W and fusion T2W/DWI in two expert observers (from 29% to 50% for observer 1 and from 23% to 50% for observer 2, respectively), reducing false positives rate[81]. To prevent unnecessary therapies in current daily practice, a strict policy for allocating patients to surgery was advocated, so the fusion of T2W with DWI could potentially prevent unnecessary adjuvant treatments, entailing more morbidity and higher costs[81].

Some authors[82] have explored the possibility of using baseline tumor ADC value as a prognostic factor for response, with conflicting results. Dashottar et al[83], in a prospective investigation, recorded significantly reduced pre-treatment ADC values in patients with locally advanced disease, resulting in no responders to radiochemotherapy. In contrast, a recent review of a large patient sample (416 patients) concluded that ADC values detected pre-therapy does not adequately correlate to radiochemotherapy

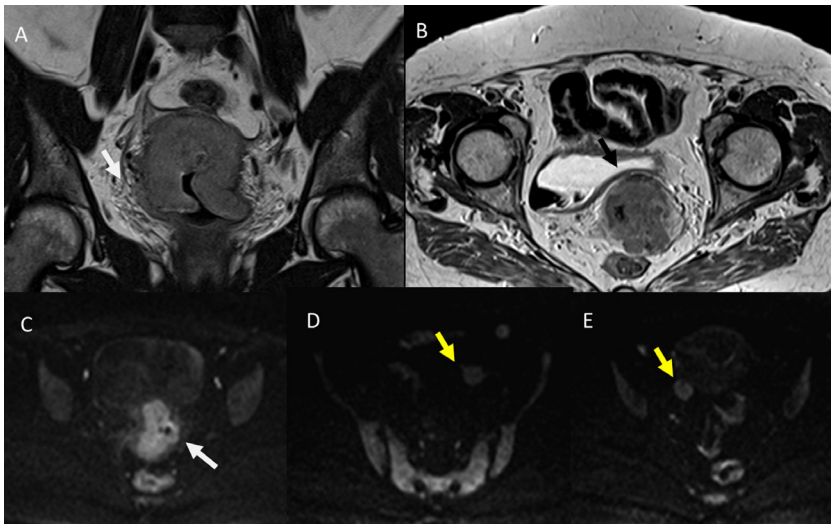

Figure 8. Conventional (1.5 T Magnetom Symphony scanner (Siemens AG, Erlangen, Germany), equipped with an 8-element body and phased array coils). **A**, TSE T2-W in the coronal plane and (**B**) TSE T1W with contrast medium in the axial plane and DWI [(**C**), b 50 s/mm^2, (**D**), b: 500 s/mm^2 and (**E**), b 800 s/mm^2) MRI assessment of CC with cervical stromal [in (**A**) white arrow], without bladder [in (**B**) black arrow] and nodes [in (**D**) and (**E**), yellow arrows] involvement. The figure was obtained by images from the Division of Radiology, "Istituto Nazionale Tumori IRCCS Fondazione Pascale – IRCCS di Napoli", Naples, Italy.

outcome for CC[83]. Harry et al[84] assumed that ADC variation during treatment could be a more reliable biomarker of the inner diffusivity change of tumor mass. In particular, a higher mean percentage increase in ADC (49.7%) within the first 3 weeks of therapy was noted in responders compared to a lower rate (19.7%) in non-responders[84]. So, the use of the change in ADC seems to be predictive of favorable therapy effect and may serve as a suitable marker for monitoring the early tumor response.

Evolution of the DWI Technique

The ADC has value in distinguishing between the degree of tumor differentiation[85], but the mono-exponential model is affected by a perfusion component and may result in errors in quantitative analysis[11,13].

IVIM could be used as a method to assess tissue diffusion and perfusion without employing any intravenous contrast agent, leading to a more faithful description of pathological processes *in vivo*[13].

Zhou et al[86] reported lower D values in less differentiated cervical tumors in 24 patients enrolled retrospectively. Despite the small sample size, interestingly, the authors proposed that regions of interest drawn at the edge of the tumor allow a better assessment of the degree of differentiation than the entire volume, when considering perfusion parameter *f*. A possible explanation was that, in less differentiated lesions, cell proliferation often exceeds tumor angiogenesis, resulting in poorly perfused central areas, leading to tumor heterogeneity for each pathological grade[86].

Besides IVIM, other models also seem to be good predictors of tumor differentiation. Winfield et al[87] in 42 CC patients evaluated retrospectively different

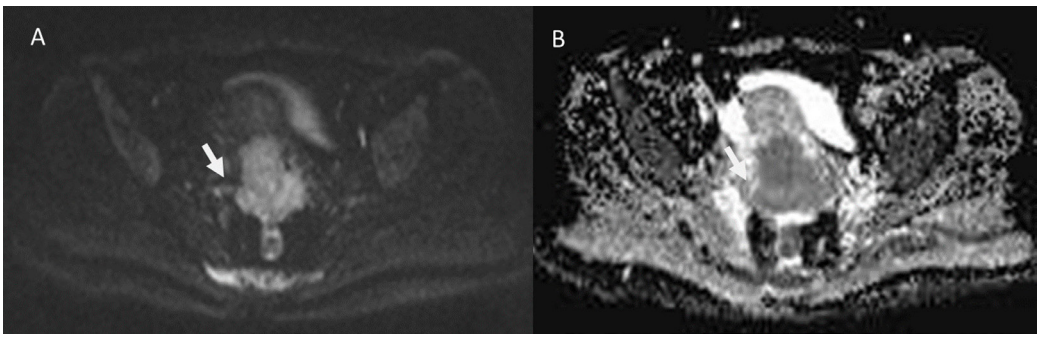

Figure 9. DWI-MRI [1.5 T Magnetom Symphony scanner (Siemens AG, Erlangen, Germany), equipped with an 8-element body and phased array coils]. **A**, b 800 s/mm^2; (**B**), ADC map [MRI assessment of CC with cervical stromal involvement (arrows)]. The lesion shows a hyperintense signal with a restricted signal in DWI [(**A**) b 800 s/mm^2) and a hypointense signal in ADC map (**B**). The figure was obtained by images from the Division of Radiology, "Istituto Nazionale Tumori IRCCS Fondazione Pascale – IRCCS di Napoli", Naples, Italy.

non-Gaussian models by comparing them with a mono-exponential model. While diffusion coefficients, including ADC, were shown to correlate similarly with tumor grade, other parameters from the non-mono-exponential models (α, K, *f*, D*) provided further information that identified tumor subtypes[87].

Different subtypes of CC have different prognoses, with varying degrees of resistance to therapy. In particular, adenocarcinoma (ACA) shows a 15-30% reduced 5-year overall survival rate compared to squamous cell carcinoma (SCC) at all stages, with increased radio- and chemoresistance[88]. Wang et al[88] reported that MD based on the DKI model in SCC was significantly lower than that in ACA, and the lower MD in CC was likely related to the restriction of free water diffusion in a more cellular-packed tumor environment.

Concurrent chemoradiation (CCRT) is recommended for bulky lesions and locally advanced CC (LACC), and the *f* and D* IVIM parameters seem to be able to monitor tumor changes during treatment[89]. According to this evidence, Perucho et al[89], found preconcurrent chemoradiotherapy (pre-CCRT) *f* values to be significantly higher in patients with partial response compared to those with stable disease or disease progression, with good observer repeatability. Conversely, it was observed that D was not significantly different between treatment groups, as instead found by Zhang et al[90] in responders, who demonstrated pre-CCRT values significantly lower. From the perspective of personalized medicine, discerning subsets of patients with poor response to standard treatment is crucial for the correct management, and future evidence is required in this field of research[91].

DCE

In recent years, conization has become a different way to obtain the diagnosis in the early stage of CC. Free resection margins after this procedure may be sufficient in selected population (Stage IA1 squamous cell tumors), mostly for fertility-sparing reasons[92,93].

DCE quantitative parameters could be useful in detecting MRI invisible residual cancer[94,95], guiding a subsequent radical hysterectomy, if required[95]. Huang et al[95] observed Ktrans and Ve values significantly higher in cancerous remnants than in their counterparts; this may reflect the loss of endothelial cell adhesion and the increased transportation of contrast agents in malignant tissue. Elevated Ktrans values would also appear to correlate with incomplete response to neoadjuvant chemotherapy (NACT) in locally advanced disease (FIGO stage IB3-IVA)[96]. The rationale of NACT is to decrease the primary tumor burden by allowing or facilitating operability and eradication of micrometastatic foci of disease[97,98]. However, the role of hysterectomy after NACT is under debate, and some centers may opt for conservative treatment in case of a complete response[99-101]. Thus, detecting tumor residuals is certainly topical (Figure 10); considering the poor reliability of morphological sequences in

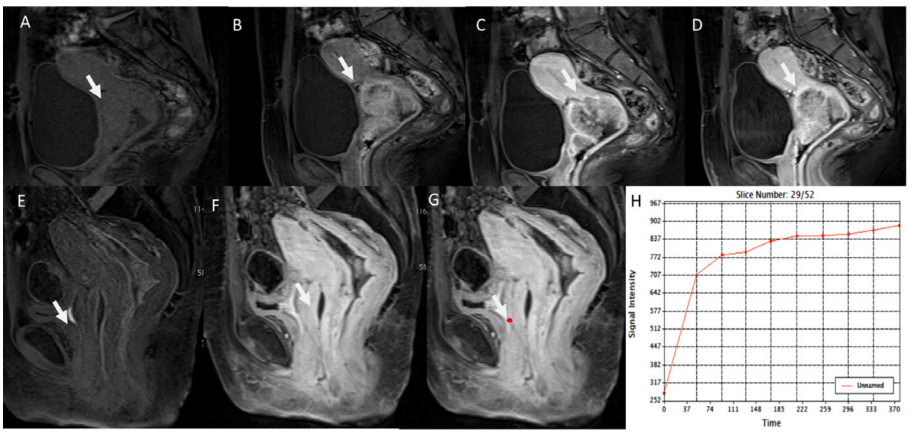

Figure 10. DCE-MRI (A 1.5 T Magnetom Symphony scanner (Siemens AG, Erlangen, Germany), equipped with an 8-element body and phased array coils) assessment of CC (white arrows). Dynamic evaluation [(**A-E**), T1W VIBE FS without contrast medium pre and post treatment; (**B**), T1-W VIBE FS in the arterial phase (45 sec); (**C-F**), T1-W Vibe FS during venous phase (90 sec) pre and post treatment and (**D-G**), T1-W vibe in the late phase (120 sec) pre and post-treatment. Before treatment, the lesion shows arterial hyperenhancement with wash-out. Complete response (arrows) after neoadjuvant treatment as demonstrated by type I curve (**H**). We employed the Gd-BT-DO3A (Gadovist, Bayer Schering Pharma AG, Berlin, German). The patient received 0.1 ml/kg of Gd-BT-DO3A by means of a power injector (Spectris Solaris® EP MR, MEDRAD Inc., Indianola, IA, USA), at an infusion rate of 2 ml/s. The figure was obtained by images from the Division of Radiology, "Istituto Nazionale Tumori IRCCS Fondazione Pascale – IRCCS di Napoli", Naples, Italy.

Table II. Functional studies in CC.

Authors	Tumor	Functional Assessment	Results
Park et al[79]	Cervical	Conventional DWI	Lower ADC values of cervical lesions for pathologic parametrial involvement
Nakamura et al[80]	Cervical	Conventional DWI	Lower ADC values of cervical lesions for pathologic parametrial involvement
Dashottar et al[83]	Cervical	Conventional DWI	Lower ADC in pre-treatment phase is correlated with poor response
Harry et al[84]	Cervical	Conventional	Higher mean percentage increase in ADC (49.7%) within the first 3 weeks of therapy was noted in responders
Zhou et al[86]	Cervical	IVIM	Lower D values correlated with less differentiated cervical tumors
Wang et al[88]	Cervical	DKI	MD was correlated with hystological sub-type
Perucho et al[89]	Cervical	IVIM	Pre-CCRT f values to be significantly higher in patients with partial response compared to those with stable disease or disease progression
Zhang et al[90]	Cervical	IVIM	Pre-CCRT diffusivity values significantly lower in responders
Jalaguier-Coudray et al[96]	Cervical	DCE-MRI	Difference between NACT responders and non-responders on DCE qualitative analysis

ADC: Apparent Diffusion coefficient; AUC: area under curve; DCE: Dynamic Contrast Enhanced; MD mean diffusivity; MK mean of Kurtosis; NACT: neoadjuvant chemotherapy; pre-CCRT: preconcurrent chemoradiotherapy.

these cases due to the inflammatory and edematous tissue changes, functional imaging could be decisive. Jalaguier-Coudray et al[96] observed a difference between NACT responders and non-responders on DCE qualitative analysis.

A time-signal intensity curve steeper than that of the myometrium, defined as "time-signal intensity curve type B"[102], showed a significant association with incomplete response. It has been suggested that DCE-MRI could be used as an indirect method to detect hypoxic areas in tumors, providing information on vascular microenvironment[96]. Tumor hypoxia could be a major cause of treatment failure in patients LACC[103].

Concerning DCE analysis based on signal intensity *vs.* time (SITC) curves, two parameters were found to be markers of tumor hypoxia: the low-expanding tumor volume (LETV) and tumor volume with increasing signal (TVIS)[103]. The LETV represents the tumor volume that shows a low contrast enhancement during the first 60 s, while TVIS refers to the volume showing contrast enhancement during a 6-minute interval, 3 to 9 minutes after contrast agent administration[103]. Both parameters resulted in prognostic factors for disease-free survival (DFS) and overall survival (OS) in LACC[103].

Research[103-116] also focused on pharmacokinetic models, which are considered more stable as they are built on the basis of physiological and biological properties of the imaged tissue. According to Halle et al[105], DCE could identify patients with hypoxia-related chemoresistance by correlating hypoxia-related genes with the Brix's model-derived parameter (ABrix), also known to measure the extravascular extracellular space. In order to compare the Brix and Tofts models on patients with CC, Andersen et al[106] concluded that low values of Ktrans and ABrix could be both representative of poor outcomes in LACC. In line with previous data, Lund et al[103] in eighty LACC patients given cisplatin-based chemoradiotherapy recorded poor disease-free survival DFS and OS in association with lower values of Ktrans. However, considering the TVIS and LETV measured in the same sample, the authors observed the majority of the patients stratified into the same risk group by the model-based and non-model-based analysis[103]. Albeit attractive, the prognostic power of Tofts and Brix-derivated biomarkers does not diverge enough from values identified by non-model-based analyses.

Consequently, it is possible that biomarkers for personalized therapy of CC could be derived by DCE-MRI without demanding image analysis on time-consuming pharmacokinetic models.

In Table II are reported the relevant functional studies in CC.

Conclusions

MRI plays a key role in the evaluation of endometrial and cervical cancer. In this scenario, it is clear as for risk assessment and pre-treatment planning, MRI should be part of the diagnostic patient approach and also as a surveillance tool in a subset of patients. In addition to morphological sequences, international guidelines recommend functional evaluation, such as DWI and DCE, for local staging of EC and CC, allowing for quantitative analysis of tumor biology and the microenvironment. In an effort of a more accurate description of physiologic and pathologic characteristics of tissues, other DWI models have been developed, with promising results[117-141]. However, a significant proportion of the parameters identified are still far from a clinical routine application, largely due to the time-consuming calculations to extract data and small sample size reports. Large multicenter prospective studies are required to determine whether these new techniques could be used to intercept optimized and personalized therapies for patients with endometrial and cervical cancer.

Ethics Approval
Not applicable.

Availability of Data and Materials
Data are reported in the manuscript.

Conflict of Interests
The authors declare no conflict of interest.

Funding
No funding was received for the study.

Authors' Contributions
FDM, RF, IS, FG, RG, MCB, LR, NM, RDA, FG, MG, and VG wrote and revised the manuscript. Each author approved the final version of the manuscript.

Acknowledgments
The authors are grateful to Alessandra Trocino, librarian at the National Cancer Institute of Naples, Italy.

References

1) Sung H, Ferlay J, Siegel RL, Laversanne M, Soerjomataram I, Jemal A, Bray F. Global Cancer Statistics 2020: GLOBOCAN Estimates of Incidence and Mortality Worldwide for 36 Cancers in 185 Countries. CA Cancer J Clin 2021; 71: 209-249.
2) Maheshwari E, Nougaret S, Stein EB, Rauch GM, Hwang KP, Stafford RJ, Klopp AH, Soliman PT, Maturen KE, Rockall AG, Lee SI, Sadowski EA, Venkatesan AM. Update on MRI in Evaluation and Treatment of Endometrial Cancer. Radiographics 2022; 42: 2112-2130.
3) Halefoglu AM, Ozagari AA. Tumor grade estımatıon of clear cell and papıllary renal cell carcınomas usıng contrast-enhanced MDCT and FSE T2 weıghted MR ımagıng: radıology-pathology correlatıon. Radiol Med 2021; 126: 1139-1148.
4) Granata V, Grassi R, Fusco R, Setola SV, Belli A, Ottaiano A, Nasti G, La Porta M, Danti G, Cappabianca S, Cutolo C, Petrillo A, Izzo F. Intrahepatic cholangiocarcinoma and its differential diagnosis at MRI: how radiologist should assess MR features. Radiol Med 2021; 126: 1584-1600.
5) Granata V, Fusco R, De Muzio F, Cutolo C, Setola SV, Dell'Aversana F, Grassi F, Belli A, Silvestro L, Ottaiano A, Nasti G, Avallone A, Flammia F, Miele V, Tatangelo F, Izzo F, Petrillo A. Radiomics and machine learning analysis based on magnetic resonance imaging in the assessment of liver mucinous colorectal metastases. Radiol Med 2022; 127: 763-772.
6) Chiloiro G, Cusumano D, de Franco P, Lenkowicz J, Boldrini L, Carano D, Barbaro B, Corvari B, Dinapoli N, Giraffa M, Meldolesi E, Manfredi R, Valentini V, Gambacorta MA. Does restaging MRI radiomics analysis improve pathological complete response prediction in rectal cancer patients? A prognostic model development. Radiol Med 2022; 127: 11-20.
7) Voicu IP, Pravatà E, Panara V, Navarra R, Mattei PA, Caulo M. Differentiating solitary brain metastases from high-grade gliomas with MR: comparing qualitative versus quantitative diagnostic strategies. Radiol Med 2022; 127: 891-898.
8) Danti G, Flammia F, Matteuzzi B, Cozzi D, Berti V, Grazzini G, Pradella S, Recchia L, Brunese L, Miele V. Gastrointestinal neuroendocrine neoplasms (GI-NENs): hot topics in morphological, functional, and prognostic imaging. Radiol Med 2021; 126: 1497-1507.
9) Renzulli M, Brandi N, Argalia G, Brocchi S, Farolfi A, Fanti S, Golfieri R. Morphological, dynamic and functional characteristics of liver pseudolesions and benign lesions. Radiol Med 2022; 127: 129-144.
10) Pasqualetti F, Malfatti G, Cantarella M, Gonnelli A, Montrone S, Montemurro N, Gadducci G, Giannini N, Pesaresi I, Perrini P, Morganti R, Cosottini M, Paiar F. Role of magnetic resonance imaging following postoperative radiotherapy in clinical decision-making of patients with high-grade glioma. Radiol Med 2022; 127: 803-808.
11) Granata V, Fusco R, Amato DM, Albino V, Patrone R, Izzo F, Petrillo A. Beyond the vascular profile: conventional DWI, IVIM and kurtosis in the assessment of hepatocellular carcinoma. Eur Rev Med Pharmacol Sci 2020; 24: 7284-7293.

12) Granata V, Fusco R, Sansone M, Grassi R, Maio F, Palaia R, Tatangelo F, Botti G, Grimm R, Curley S, Avallone A, Izzo F, Petrillo A. Magnetic resonance imaging in the assessment of pancreatic cancer with quantitative parameter extraction by means of dynamic contrast-enhanced magnetic resonance imaging, diffusion kurtosis imaging and intravoxel incoherent motion diffusion-weighted imaging. Therap Adv Gastroenterol 2020; 13: 1756284819885052.
13) Borgheresi A, De Muzio F, Agostini A, Ottaviani L, Bruno A, Granata V, Fusco R, Danti G, Flammia F, Grassi R, Grassi F, Bruno F, Palumbo P, Barile A, Miele V, Giovagnoni A. Lymph Nodes Evaluation in Rectal Cancer: Where Do We Stand and Future Perspective. J Clin Med 2022; 11: 2599.
14) Granata V, Fusco R, Belli A, Danti G, Bicci E, Cutolo C, Petrillo A, Izzo F. Diffusion weighted imaging and diffusion kurtosis imaging in abdominal oncological setting: why and when. Infect Agent Cancer 2022; 17: 25.
15) Albano D, Bruno F, Agostini A, Angileri SA, Benenati M, Bicchierai G, Cellina M, Chianca V, Cozzi D, Danti G, De Muzio F, Di Meglio L, Gentili F, Giacobbe G, Grazzini G, Grazzini I, Guerriero P, Messina C, Micci G, Palumbo P, Rocco MP, Grassi R, Miele V, Barile A; Young SIRM Working Group. Dynamic contrast-enhanced (DCE) imaging: state of the art and applications in whole-body imaging. Jpn J Radiol 2022; 40: 341-366.
16) Bordonaro V, Ciancarella P, Ciliberti P, Curione D, Napolitano C, Santangelo TP, Natali GL, Rollo M, Guccione P, Pasquini L, Secinaro A. Dynamic contrast-enhanced magnetic resonance lymphangiography in pediatric patients with central lymphatic system disorders. Radiol Med 2021; 126: 737-743.
17) Fusco R, Granata V, Sansone M, Rega D, Delrio P, Tatangelo F, Romano C, Avallone A, Pupo D, Giordano M, Grassi R, Ravo V, Pecori B, Petrillo A. Validation of the standardized index of shape tool to analyze DCE-MRI data in the assessment of neo-adjuvant therapy in locally advanced rectal cancer. Radiol Med 2021; 126: 1044-1054.
18) Ahmed Z, Levesque IR. Pharmacokinetic modeling of dynamic contrast-enhanced MRI using a reference region and input function tail. Magn Reson Med 2020; 83: 286-298.
19) Dappa E, Elger T, Hasenburg A, Düber C, Battista MJ, Hötker AM. The value of advanced MRI techniques in the assessment of cervical cancer: a review. Insights Imaging 2017; 8: 471-481.
20) Oaknin A, Bosse TJ, Creutzberg CL, Giornelli G, Harter P, Joly F, Lorusso D, Marth C, Makker V, Mirza MR, Ledermann JA, Colombo N; ESMO Guidelines Committee. Electronic address: clinicalguidelines@esmo.org. Endometrial cancer: ESMO Clinical Practice Guideline for diagnosis, treatment and follow-up. Ann Oncol 2022; 33: 860-877.
21) Bokhman JV. Two pathogenetic types of endometrial carcinoma. Gynecol Oncol 1983; 15: 10-17.
22) Prat J, Gallardo A, Cuatrecasas M, Catasús L. Endometrial carcinoma: pathology and genetics. Pathology 2007; 39: 72-87.
23) Llobet D, Pallares J, Yeramian A, Santacana M, Eritja N, Velasco A, Dolcet X, Matias-Guiu X. Molecular pathology of endometrial carcinoma: practical aspects from the diagnostic and therapeutic viewpoints. J Clin Pathol 2009; 62: 777-785.
24) Kasius JC, Pijnenborg JMA, Lindemann K, Forsse D, van Zwol J, Kristensen GB, Krakstad C, Werner HMJ, Amant F. Risk Stratification of Endometrial Cancer Patients: FIGO Stage, Biomarkers and Molecular Classification. Cancers (Basel) 2021; 13: 5848.
25) Park JJ, Kim CK, Cho SW, Kim JH. Utility of diffusion-weighted imaging in association with pathologic upgrading in biopsy-proven grade I endometrial cancer. J Magn Reson Imaging 2020; 51: 117-123.
26) Xu X, Li H, Wang S, Fang M, Zhong L, Fan W, Dong D, Tian J, Zhao X. Multiplanar MRI-Based Predictive Model for Preoperative Assessment of Lymph Node Metastasis in Endometrial Cancer. Front Oncol 2019; 9:1007.
27) Cellina M, Gibelli D, Martinenghi C, Giardini D, Soresina M, Menozzi A, Oliva G, Carrafiello G. Non-contrast magnetic resonance lymphography (NCMRL) in cancer-related secondary lymphedema: acquisition technique and imaging findings. Radiol Med 2021; 126: 1477-1486.
28) Zhang Q, Ouyang H, Ye F, Chen S, Xie L, Zhao X, Yu X. Multiple mathematical models of diffusion-weighted imaging for endometrial cancer characterization: Correlation with prognosis-related risk factors. Eur J Radiol 2020; 130: 109102.
29) Qin H, Que Q, Lin P, Li X, Wang XR, He Y, Chen JQ, Yang H. Magnetic resonance imaging (MRI) radiomics of papillary thyroid cancer (PTC): a comparison of predictive performance of multiple classifiers modeling to identify cervical lymph node metastases before surgery. Radiol Med 2021; 126: 1312-1327.
30) Nougaret S, Reinhold C, Alsharif SS, Addley H, Arceneau J, Molinari N, Guiu B, Sala E. Endometrial Cancer: Combined MR Volumetry and Diffusion-weighted Imaging for Assessment of Myometrial and Lymphovascular Invasion and Tumor Grade. Radiology 2015; 276: 797-808.
31) Inoue C, Fujii S, Kaneda S, Fukunaga T, Kaminou T, Kigawa J, Harada T, Ogawa T. Correlation of apparent diffusion coefficient value with prognostic parameters of endometrioid carcinoma. J Magn Reson Imaging 2015; 41: 213-219.
32) Woo S, Cho JY, Kim SY, Kim SH. Histogram analysis of apparent diffusion coefficient map of diffusion-weighted MRI in endometrial cancer: a preliminary correlation study with histological grade. Acta Radiol 2014; 55: 1270-1277.
33) Yan B, Zhao T, Liang X, Niu C, Ding C. Can the apparent diffusion coefficient differentiate the grade of endometrioid adenocarcinoma and the histological subtype of endometrial cancer? Acta Radiol 2018; 59: 363-370.
34) Reyes-Pérez JA, Villaseñor-Navarro Y, Jiménez de Los Santos ME, Pacheco-Bravo I, Calle-Loja M, Sollozo-Dupont I. The apparent diffusion coefficient (ADC) on 3-T MRI differentiates myometrial invasion depth and histological grade in patients with endometrial cancer. Acta Radiol 2020; 61: 1277-1286.

35) Ozturk M, Kalkan C, Danaci M, Kefeli M. Diffusion-weighted MRI at 3T in Endometrial Cancer: Correlation of Apparent Diffusion Coefficient with Histopathological Prognostic Parameters. J Coll Physicians Surg Pak 2021; 31: 1399-1405.
36) Chen J, Fan W, Gu H, Wang Y, Liu Y, Chen X, Ren S, Wang Z. The value of the apparent diffusion coefficient in differentiating type II from type I endometrial carcinoma. Acta Radiol 2021; 62: 959-965.
37) Helpman L, Kupets R, Covens A, Saad RS, Khalifa MA, Ismiil N, Ghorab Z, Dubé V, Nofech-Mozes S. Assessment of endometrial sampling as a predictor of final surgical pathology in endometrial cancer. Br J Cancer 2014; 110: 609-615.
38) Nougaret S, Horta M, Sala E, Lakhman Y, Thomassin-Naggara I, Kido A, Masselli G, Bharwani N, Sadowski E, Ertmer A, Otero-Garcia M, Kubik-Huch RA, Cunha TM, Rockall A, Forstner R. Endometrial Cancer MRI staging: Updated Guidelines of the European Society of Urogenital Radiology. Eur Radiol 2019; 29: 792-805.
39) Song Y, Shang H, Ma Y, Li X, Jiang J, Geng Z, Shang J. Can conventional DWI accurately assess the size of endometrial cancer? Abdom Radiol (NY) 2020; 45: 1132-1140.
40) Ota T, Hori M, Onishi H, Sakane M, Tsuboyama T, Tatsumi M, Nakamoto A, Kimura T, Narumi Y, Tomiyama N. Preoperative staging of endometrial cancer using reduced field-of-view diffusion-weighted imaging: a preliminary study. Eur Radiol 2017; 27: 5225-5235.
41) Guo Y, Wang P, Wang P, Gao W, Li F, Yang X, Ni H, Shen W, Guo Z. Myometrial invasion and overall staging of endometrial carcinoma: assessment using fusion of T2-weighted magnetic resonance imaging and diffusion-weighted magnetic resonance imaging. Onco Targets Ther 2017; 10: 5937-5943.
42) Andreano A, Rechichi G, Rebora P, Sironi S, Valsecchi MG, Galimberti S. MR diffusion imaging for preoperative staging of myometrial invasion in patients with endometrial cancer: a systematic review and meta-analysis. Eur Radiol 2014; 24: 1327-1338.
43) Deng L, Wang QP, Chen X, Duan XY, Wang W, Guo YM. The Combination of Diffusion- and T2-Weighted Imaging in Predicting Deep Myometrial Invasion of Endometrial Cancer: A Systematic Review and Meta-Analysis. J Comput Assist Tomogr 2015; 39: 661-673.
44) Granata V, Bicchierai G, Fusco R, Cozzi D, Grazzini G, Danti G, De Muzio F, Maggialetti N, Smorchkova O, D'Elia M, Brunese MC, Grassi R, Giacobbe G, Bruno F, Palumbo P, Grassi F, Brunese L, Grassi R, Miele V, Barile A. Diagnostic protocols in oncology: workup and treatment planning. Part 2: Abbreviated MR protocol. Eur Rev Med Pharmacol Sci; 25: 6499-6528.
45) Stanzione A, Maurea S, Danzi R, Cuocolo R, Galatola R, Romeo V, Raffone A, Travaglino A, Di Spiezio Sardo A, Insabato L, Pace L, Scaglione M, Brunetti A, Mainenti PP. MRI to assess deep myometrial invasion in patients with endometrial cancer:A multi-reader study to evaluate the diagnostic role of different sequences. Eur J Radiol 2021; 138: 109629.
46) Shannon BA, Ahlawat S, Morris CD, Levin AS, Fayad LM. Do contrast-enhanced and advanced MRI sequences improve diagnostic accuracy for indeterminate lipomatous tumors? Radiol Med 2022; 127: 90-99.
47) Scialpi M, Scialpi P, Martorana E, Torre R, Mancioli FA, D'Andrea A, Di Blasi A. Biparametric MRI with simplified PI-RADS (S-PI-RADS) for prostate cancer detection and management: what do radiologist need to know. Radiol Med 2021; 126: 1660-1661.
48) Chryssou EG, Manikis GC, Ioannidis GS, Chaniotis V, Vrekoussis T, Maris TG, Marias K, Karantanas AH. Diffusion Weighted Imaging in the Assessment of Tumor Grade in Endometrial Cancer Based on Intravoxel Incoherent Motion MRI. Diagnostics (Basel) 2022; 12: 692.
49) Orsatti G, Zucchetta P, Varotto A, Crimì F, Weber M, Cecchin D, Bisogno G, Spimpolo A, Giraudo C, Stramare R. Volumetric histograms-based analysis of apparent diffusion coefficients and standard uptake values for the assessment of pediatric sarcoma at staging: preliminary results of a PET/MRI study. Radiol Med 2021; 126: 878-885.
50) Chen T, Li Y, Lu SS, Zhang YD, Wang XN, Luo CY, Shi HB. Quantitative evaluation of diffusion-kurtosis imaging for grading endometrial carcinoma: a comparative study with diffusion-weighted imaging. Clin Radiol 2017; 72: 995.e11-995.e20.
51) Yue W, Meng N, Wang J, Liu W, Wang X, Yan M, Han D, Cheng J. Comparative analysis of the value of diffusion kurtosis imaging and diffusion-weighted imaging in evaluating the histological features of endometrial cancer. Cancer Imaging 2019; 19: 9.
52) Braun MM, Overbeek-Wager EA, Grumbo RJ. Diagnosis and Management of Endometrial Cancer. Am Fam Physician 2016; 93: 468-474.
53) Takeuchi M, Matsuzaki K, Nishitani H. Diffusion-weighted magnetic resonance imaging of endometrial cancer: differentiation from benign endometrial lesions and preoperative assessment of myometrial invasion. Acta Radiol 2009; 50: 947-953.
54) Alektiar KM, McKee A, Lin O, Venkatraman E, Zelefsky MJ, Mychalczak BR, McKee B, Hoskins WJ, Barakat RR. The significance of the amount of myometrial invasion in patients with Stage IB endometrial carcinoma. Cancer 2002; 95: 316-321.
55) Song JC, Lu SS, Zhang J, Liu XS, Luo CY, Chen T. Quantitative assessment of diffusion kurtosis imaging depicting deep myometrial invasion: a comparative analysis with diffusion-weighted imaging. Diagn Interv Radiol 2020; 26: 74-81.
56) Bennett KM, Schmainda KM, Bennett RT, Rowe DB, Lu H, Hyde JS. Characterization of continuously distributed cortical water diffusion rates with a stretched-exponential model. Magn Reson Med 2003; 50: 727-734.
57) Pace C, Argirò R, Casadei L, Cesareni M, Orlacchio A. Comparison between X-ray-hysterosalpingography and 3 Tesla magnetic resonance-hysterosalpingography in the assessment of the tubal patency in the cause of female infertility. Radiol Med 2022; 127: 1373-1382.
58) Nurdillah I, Rizuana IH, Suraya A, Syazarina SO. A Comparison of Dynamic Contrast-Enhanced Magnetic Resonance Imaging and T2-Weighted

Imaging in Determining the Depth of Myometrial Invasion in Endometrial Carcinoma-A Retrospective Study. J Pers Med 2022; 12: 1268.
59) Nougaret S, Lakhman Y, Vargas HA, Colombo PE, Fujii S, Reinhold C, Sala E. From Staging to Prognostication: Achievements and Challenges of MR Imaging in the Assessment of Endometrial Cancer. Magn Reson Imaging Clin N Am 2017; 25: 611-633.
60) Freeman SJ, Aly AM, Kataoka MY, Addley HC, Reinhold C, Sala E. The revised FIGO staging system for uterine malignancies: implications for MR imaging. Radiographics 2012; 32: 1805-1827.
61) Bi Q, Chen Y, Chen J, Zhang H, Lei Y, Yang J, Zhang Y, Bi G. Predictive value of T2-weighted imaging and dynamic contrast-enhanced MRI for assessing cervical invasion in patients with endometrial cancer: a meta-analysis. Clin Imaging 2021; 78: 206-213.
62) Bhatla N, Aoki D, Sharma DN, Sankaranarayanan R. Cancer of the cervix uteri. Int J Gynaecol Obstet 2018; 143: 22-36.
63) Marth C, Landoni F, Mahner S, McCormack M, Gonzalez-Martin A, Colombo N; ESMO Guidelines Committee. Cervical cancer: ESMO Clinical Practice Guidelines for diagnosis, treatment and follow-up. Ann Oncol 2017; 28: iv72-iv83.
64) Bhatla N, Berek JS, Cuello Fredes M, Denny LA, Grenman S, Karunaratne K, Kehoe ST, Konishi I, Olawaiye AB, Prat J, Sankaranarayanan R, Brierley J, Mutch D, Querleu D, Cibula D, Quinn M, Botha H, Sigurd L, Rice L, Ryu HS, Ngan H, Mäenpää J, Andrijono A, Purwoto G, Maheshwari A, Bafna UD, Plante M, Natarajan J. Revised FIGO staging for carcinoma of the cervix uteri. Int J Gynaecol Obstet 2019; 145: 129-135.
65) Fournier LS, Bats AS, Durdux C. Diffusion MRI: Technical principles and application to uterine cervical cancer. Cancer Radiother 2020; 24: 368-373.
66) Singh N, Arif S. Histopathologic parameters of prognosis in cervical cancer--a review. Int J Gynecol Cancer 2004; 14: 741-750.
67) Katanyoo K, Sanguanrungsirikul S, Manusirivithaya S. Comparison of treatment outcomes between squamous cell carcinoma and adenocarcinoma in locally advanced cervical cancer. Gynecol Oncol 2012; 125: 292-296.
68) Chiti G, Grazzini G, Flammia F, Matteuzzi B, Tortoli P, Bettarini S, Pasqualini E, Granata V, Busoni S, Messserini L, Pradella S, Massi D, Miele V. Gastroenteropancreatic neuroendocrine neoplasms (GEP-NENs): a radiomic model to predict tumor grade. Radiol Med 2022; 127: 928-938.
69) Manganaro L, Lakhman Y, Bharwani N, Gui B, Gigli S, Vinci V, Rizzo S, Kido A, Cunha TM, Sala E, Rockall A, Forstner R, Nougaret S. Staging, recurrence and follow-up of uterine cervical cancer using MRI: Updated Guidelines of the European Society of Urogenital Radiology after revised FIGO staging 2018. Eur Radiol 2021; 31: 7802-7816.
70) Xue K, Liu L, Liu Y, Guo Y, Zhu Y, Zhang M. Radiomics model based on multi-sequence MR images for predicting preoperative immunoscore in rectal cancer. Radiol Med 2022; 127: 702-713.
71) Cipollari S, Pecoraro M, Forookhi A, Laschena L, Bicchetti M, Messina E, Lucciola S, Catalano C, Panebianco V. Biparametric prostate MRI: impact of a deep learning-based software and of quantitative ADC values on the inter-reader agreement of experienced and inexperienced readers. Radiol Med 2022; 127: 1245-1253.
72) Manoharan D, Das CJ, Aggarwal A, Gupta AK. Diffusion weighted imaging in gynecological malignancies - present and future. World J Radiol 2016; 8: 288-297.
73) Lo Casto A, Cannella R, Taravella R, Cordova A, Matta D, Campisi G, Attanasio M, Rinaldi G, Rodolico V. Diagnostic and prognostic value of magnetic resonance imaging in the detection of tumor depth of invasion and bone invasion in patients with oral cavity cancer. Radiol Med 2022; 127: 1364-1372.
74) Hwang J, Hong SS, Kim HJ, Chang YW, Nam BD, Oh E, Lee E, Cha H. Reduced field-of-view diffusion-weighted MRI in patients with cervical cancer. Br J Radiol 2018; 91: 20170864.
75) Chen M, Feng C, Wang Q, Li J, Wu S, Hu D, Deng B, Li Z. Comparison of reduced field-of-view diffusion-weighted imaging (DWI) and conventional DWI techniques in the assessment of Cervical carcinoma at 3.0T: Image quality and FIGO staging. Eur J Radiol 2021; 137: 109557.
76) Assadsangabi R, Babaei R, Songco C, Ivanovic V, Bobinski M, Chen YJ, Nabavizadeh SA. Multimodality oncologic evaluation of superficial neck and facial lymph nodes. Radiol Med 2021; 126: 1074-1084.
77) Xue HD, Li S, Sun F, Sun HY, Jin ZY, Yang JX, Yu M. Clinical application of body diffusion weighted MR imaging in the diagnosis and preoperative N staging of cervical cancer. Chin Med Sci J 2008; 23: 133-137.
78) Lin G, Ho KC, Wang JJ, Ng KK, Wai YY, Chen YT, Chang CJ, Ng SH, Lai CH, Yen TC. Detection of lymph node metastasis in cervical and uterine cancers by diffusion-weighted magnetic resonance imaging at 3T. J Magn Reson Imaging 2008; 28: 128-135.
79) Park JJ, Kim CK, Park SY, Park BK, Kim B. Value of diffusion-weighted imaging in predicting parametrial invasion in stage IA2-IIA cervical cancer. Eur Radiol 2014; 24: 1081-1088.
80) Nakamura K, Joja I, Nagasaka T, Fukushima C, Kusumoto T, Seki N, Hongo A, Kodama J, Hiramatsu Y. The mean apparent diffusion coefficient value (ADCmean) on primary cervical cancer is a predictive marker for disease recurrence. Gynecol Oncol 2012; 127: 478-483.
81) Mongula JE, Bakers FCH, Mihl C, van Gorp T, Kruitwagen RFPM, Slangen BFM. Assessment of parametrial invasion of cervical carcinoma, the role of T2-weighted MRI and diffusion weighted imaging with or without fusion. Clin Radiol 2019; 74: 790-796.
82) Yang W, Qiang JW, Tian HP, Chen B, Wang AJ, Zhao JG. Multi-parametric MRI in cervical cancer: early prediction of response to concurrent chemoradiotherapy in combination with clinical prognostic factors. Eur Radiol 2018; 28: 437-445.
83) Dashottar S, Preeth Pany T, Lohia N. Role of apparent diffusion coefficient as a biomarker in the evaluation of cervical cancer. Indian J Radiol Imaging 2019; 29: 25-32.

84) Harry VN, Persad S, Bassaw B, Parkin D. Diffusion-weighted MRI to detect early response to chemoradiation in cervical cancer: A systematic review and meta-analysis. Gynecol Oncol Rep 2021; 38: 100883.
85) Xue H, Ren C, Yang J, Sun Z, Li S, Jin Z, Shen K, Zhou W. Histogram analysis of apparent diffusion coefficient for the assessment of local aggressiveness of cervical cancer. Arch Gynecol Obstet 2014; 290: 341-348.
86) Zhou Y, Liu J, Liu C, Jia J, Li N, Xie L, Zhou Z, Zhang Z, Zheng D, He W, Shen Y, Lu W, Zhu H. Intravoxel incoherent motion diffusion weighted MRI of cervical cancer - Correlated with tumor differentiation and perfusion. Magn Reson Imaging 2016; 34: 1050-1056.
87) Winfield JM, Orton MR, Collins DJ, Ind TE, Attygalle A, Hazell S, Morgan VA, deSouza NM. Separation of type and grade in cervical tumours using non-mono-exponential models of diffusion-weighted MRI. Eur Radiol 2017; 27: 627-636.
88) Wang M, Perucho JAU, Chan Q, Sun J, Ip P, Tse KY, Lee EYP. Diffusion Kurtosis Imaging in the Assessment of Cervical Carcinoma. Acad Radiol 2020; 27: e94-e101.
89) Perucho JAU, Wang M, Vardhanabhuti V, Tse KY, Chan KKL, Lee EYP. Association between IVIM parameters and treatment response in locally advanced squamous cell cervical cancer treated by chemoradiotherapy. Eur Radiol 2021; 31: 7845-7854.
90) Zhang H, Zhou Y, Li J, Zhang P, Li Z, Guo J. The value of DWI in predicting the response to synchronous radiochemotherapy for advanced cervical carcinoma: comparison among three mathematical models. Cancer Imaging 2020; 20: 8.
91) Granata V, Fusco R, De Muzio F, Cutolo C, Setola SV, Grassi R, Grassi F, Ottaiano A, Nasti G, Tatangelo F, Pilone V, Miele V, Brunese MC, Izzo F, Petrillo A. Radiomics textural features by MR imaging to assess clinical outcomes following liver resection in colorectal liver metastases. Radiol Med 2022; 127: 461-470.
92) Mitchell DG, Snyder B, Coakley F, Reinhold C, Thomas G, Amendola M, Schwartz LH, Woodward P, Pannu H, Hricak H. Early invasive cervical cancer: tumor delineation by magnetic resonance imaging, computed tomography, and clinical examination, verified by pathologic results, in the ACRIN 6651/GOG 183 Intergroup Study. J Clin Oncol 2006; 24: 5687-5694.
93) Chen XL, Chen GW, Xu GH, Ren J, Li ZL, Pu H, Li H. Tumor Size at Magnetic Resonance Imaging Association With Lymph Node Metastasis and Lymphovascular Space Invasion in Resectable Cervical Cancer: A Multicenter Evaluation of Surgical Specimens. Int J Gynecol Cancer 2018; 28: 1545-1552.
94) Gao W, Wang W, Song D, Yang C, Zhu K, Zeng M, Rao SX, Wang M. A predictive model integrating deep and radiomics features based on gadobenate dimeglumine-enhanced MRI for postoperative early recurrence of hepatocellular carcinoma. Radiol Med 2022; 127: 259-271.
95) Huang JW, Song JC, Chen T, Yang M, Ma ZL. Making the invisible visible: improving detectability of MRI-invisible residual cervical cancer after conisation by DCE-MRI. Clin Radiol 2019; 74: 166.e15-166.e21.
96) Jalaguier-Coudray, Aurélie; Villard-Mahjoub, Rim; Delouche, Aurélie; Delarbre, Béatrice; Lambaudie, Eric; Houvenaeghel, Gilles; Minsat, Mathieu; Tallet, Agnès; Sabatier, Renaud; Thomassin-Naggara, Isabelle.Value of Dynamic Contrast-enhanced and Diffusion-weighted MR Imaging in the Detection of Pathologic Complete Response in Cervical Cancer after Neoadjuvant Therapy: A Retrospective Observational Study. Radiology 2017: 161299.
97) Autorino R, Gui B, Panza G, Boldrini L, Cusumano D, Russo L, Nardangeli A, Persiani S, Campitelli M, Ferrandina G, Macchia G, Valentini V, Gambacorta MA, Manfredi R. Radiomics-based prediction of two-year clinical outcome in locally advanced cervical cancer patients undergoing neoadjuvant chemoradiotherapy. Radiol Med 2022; 127: 498-506.
98) Fusco R, Granata V, Sansone M, Rega D, Delrio P, Tatangelo F, Romano C, Avallone A, Pupo D, Giordano M, Grassi R, Ravo V, Pecori B, Petrillo A. Validation of the standardized index of shape tool to analyze DCE-MRI data in the assessment of neo-adjuvant therapy in locally advanced rectal cancer. Radiol Med 2021; 126: 1044-1054.
99) Morice P, Rouanet P, Rey A, Romestaing P, Houvenaeghel G, Boulanger JC, Leveque J, Cowen D, Mathevet P, Malhaire JP, Magnin G, Fondrinier E, Berille J, Haie-Meder C. Results of the GYNECO 02 study, an FNCLCC phase III trial comparing hysterectomy with no hysterectomy in patients with a (clinical and radiological) complete response after chemoradiation therapy for stage IB2 or II cervical cancer. Oncologist 2012; 17: 64-71.
100) Houvenaeghel G, Lelievre L, Buttarelli M, Jacquemier J, Carcopino X, Viens P, Gonzague-Casabianca L. Contribution of surgery in patients with bulky residual disease after chemoradiation for advanced cervical carcinoma. Eur J Surg Oncol 2007; 33: 498-503.
101) Russo L, Gui B, Miccò M, Panico C, De Vincenzo R, Fanfani F, Scambia G, Manfredi R. The role of MRI in cervical cancer>2 cm (FIGO stage IB2-IIA1) conservatively treated with neoadjuvant chemotherapy followed by conization: a pilot study. Radiol Med 2021; 126: 1055-1063.
102) Hawighorst H, Knapstein PG, Schaeffer U, Knopp MV, Brix G, Hoffmann U, Zuna I, Essig M, van Kaick G. Pelvic lesions in patients with treated cervical carcinoma: efficacy of pharmacokinetic analysis of dynamic MR images in distinguishing recurrent tumors from benign conditions. AJR Am J Roentgenol 1996; 166: 401-408.
103) Lund KV, Simonsen TG, Kristensen GB, Rofstad EK. DCE-MRI of locally-advanced carcinoma of the uterine cervix: Tofts analysis versus non-model-based analyses. Radiat Oncol 2020; 15: 79.
104) Mungai F, Verrone GB, Bonasera L, Bicci E, Pietragalla M, Nardi C, Berti V, Mazzoni LN, Miele V. Imaging biomarkers in the diagnosis of salivary gland tumors: the value of lesion/parenchyma ra-

tio of perfusion-MR pharmacokinetic parameters. Radiol Med 2021; 126: 1345-1355.
105) Halle C, Andersen E, Lando M, Aarnes EK, Hasvold G, Holden M, Syljuåsen RG, Sundfør K, Kristensen GB, Holm R, Malinen E, Lyng H. Hypoxia-induced gene expression in chemoradioresistant cervical cancer revealed by dynamic contrast-enhanced MRI. Cancer Res 2012; 72: 5285-5295.
106) Andersen EK, Hole KH, Lund KV, Sundfør K, Kristensen GB, Lyng H, Malinen E. Pharmacokinetic parameters derived from dynamic contrast enhanced MRI of cervical cancers predict chemoradiotherapy outcome. Radiother Oncol 2013; 107: 117-122.
107) Granata V, Fusco R, Risi C, Ottaiano A, Avallone A, De Stefano A, Grimm R, Grassi R, Brunese L, Izzo F, Petrillo A. Diffusion-Weighted MRI and Diffusion Kurtosis Imaging to Detect RAS Mutation in Colorectal Liver Metastasis. Cancers (Basel) 2020; 12: 2420.
108) Granata V, Fusco R, Costa M, Picone C, Cozzi D, Moroni C, La Casella GV, Montanino A, Monti R, Mazzoni F, Grassi R, Malagnino VG, Cappabianca S, Grassi R, Miele V, Petrillo A. Preliminary Report on Computed Tomography Radiomics Features as Biomarkers to Immunotherapy Selection in Lung Adenocarcinoma Patients. Cancers (Basel) 2021; 13: 3992.
109) Granata V, Fusco R, Catalano O, Setola SV, de Lutio di Castelguidone E, Piccirillo M, Palaia R, Grassi R, Granata F, Izzo F, Petrillo A. Multidetector computer tomography in the pancreatic adenocarcinoma assessment: an update. Infect Agent Cancer 2016; 11: 57.
110) Granata V, Fusco R, Avallone A, Catalano O, Piccirillo M, Palaia R, Nasti G, Petrillo A, Izzo F. A radiologist's point of view in the presurgical and intraoperative setting of colorectal liver metastases. Future Oncol 2018; 14: 2189-2206.
111) Granata V, Fusco R, Barretta ML, Picone C, Avallone A, Belli A, Patrone R, Ferrante M, Cozzi D, Grassi R, Grassi R, Izzo F, Petrillo A. Radiomics in hepatic metastasis by colorectal cancer. Infect Agent Cancer 2021; 16: 39.
112) Granata V, Fusco R, Setola SV, Picone C, Vallone P, Belli A, Incollingo P, Albino V, Tatangelo F, Izzo F, Petrillo A. Microvascular invasion and grading in hepatocellular carcinoma: correlation with major and ancillary features according to LIRADS. Abdom Radiol (NY) 2019; 44: 2788-2800.
113) Granata V, Grassi R, Fusco R, Setola SV, Palaia R, Belli A, Miele V, Brunese L, Grassi R, Petrillo A, Izzo F. Assessment of Ablation Therapy in Pancreatic Cancer: The Radiologist's Challenge. Front Oncol 2020; 10: 560952.
114) Granata V, Fusco R, Avallone A, Catalano O, Filice F, Leongito M, Palaia R, Izzo F, Petrillo A. Major and ancillary magnetic resonance features of LI-RADS to assess HCC: an overview and update. Infect Agent Cancer 2017; 12: 23.
115) Granata V, Fusco R, Catalano O, Avallone A, Palaia R, Botti G, Tatangelo F, Granata F, Cascella M, Izzo F, Petrillo A. Diagnostic accuracy of magnetic resonance, computed tomography and contrast enhanced ultrasound in radiological multimodality assessment of peribiliary liver metastases. PLoS One 2017; 12: e0179951.
116) Fusco R, Sansone M, Granata V, Grimm R, Pace U, Delrio P, Tatangelo F, Botti G, Avallone A, Pecori B, Petrillo A. Diffusion and perfusion MR parameters to assess preoperative short-course radiotherapy response in locally advanced rectal cancer: a comparative explorative study among Standardized Index of Shape by DCE-MRI, intravoxel incoherent motion- and diffusion kurtosis imaging-derived parameters. Abdom Radiol (NY) 2019; 44: 3683-3700.
117) Granata V, de Lutio di Castelguidone E, Fusco R, Catalano O, Piccirillo M, Palaia R, Izzo F, Gallipoli AD, Petrillo A. Irreversible electroporation of hepatocellular carcinoma: preliminary report on the diagnostic accuracy of magnetic resonance, computer tomography, and contrast-enhanced ultrasound in evaluation of the ablated area. Radiol Med 2016; 121: 122-131.
118) Colombo E, Fick T, Esposito G, Germans M, Regli L, van Doormaal T. Segmentation techniques of brain arteriovenous malformations for 3D visualization: a systematic review. Radiol Med 2022; 127: 1333-1341.
119) Hyodo R, Takehara Y, Naganawa S. 4D Flow MRI in the portal venous system: imaging and analysis methods, and clinical applications. Radiol Med 2022; 127: 1181-1198.
120) Zerunian M, Pucciarelli F, Caruso D, Polici M, Masci B, Guido G, De Santis D, Polverari D, Principessa D, Benvenga A, Iannicelli E, Laghi A. Artificial intelligence based image quality enhancement in liver MRI: a quantitative and qualitative evaluation. Radiol Med 2022; 127: 1098-1105.
121) Fushimi Y, Yoshida K, Okawa M, Maki T, Nakajima S, Sakata A, Okuchi S, Hinoda T, Kanagaki M, Nakamoto Y. Vessel wall MR imaging in neuroradiology. Radiol Med 2022; 127: 1032-1045.
122) Bicchetti M, Simone G, Giannarini G, Girometti R, Briganti A, Brunocilla E, Cardone G, De Cobelli F, Gaudiano C, Del Giudice F, Flammia S, Leonardo C, Pecoraro M, Schiavina R, Catalano C, Panebianco V. A novel pathway to detect muscle-invasive bladder cancer based on integrated clinical features and VI-RADS score on MRI: results of a prospective multicenter study. Radiol Med 2022; 127: 881-890.
123) Salaffi F, Carotti M, Di Carlo M, Ceccarelli L, Farah S, Giovagnoni A. The value of ultrasound and magnetic resonance imaging scoring systems in explaining handgrip strength and functional impairment in rheumatoid arthritis patients: a pilot study. Radiol Med 2022; 127: 652-663.
124) Cirillo L, Rustici A, Toni F, Zoli M, Bartiromo F, Gramegna LL, Cicala D, Tonon C, Caranci F, Lodi R. Vessel Wall MRI: clinical implementation in cerebrovascular disorders-technical aspects. Radiol Med 2022; 127: 645-651.
125) Gitto S, Bologna M, Corino VDA, Emili I, Albano D, Messina C, Armiraglio E, Parafioriti A, Luzzati A, Mainardi L, Sconfienza LM. Diffusion-weighted MRI radiomics of spine bone

tumors: feature stability and machine learning-based classification performance. Radiol Med 2022; 127: 518-525.
126) Romano A, Moltoni G, Guarnera A, Pasquini L, Di Napoli A, Napolitano A, Espagnet MCR, Bozzao A. Single brain metastasis versus glioblastoma multiforme: a VOI-based multiparametric analysis for differential diagnosis. Radiol Med 2022; 127: 490-497.
127) Orlacchio A, Guastoni C, Beretta GD, Cosmai L, Galluzzo M, Gori S, Grassedonio E, Incorvaia L, Marcantoni C, Netti GS, Passamonti M, Porta C, Procopio G, Rizzo M, Roma S, Romanini L, Stacul F, Casinelli A. SIRM-SIN-AIOM: appropriateness criteria for evaluation and prevention of renal damage in the patient undergoing contrast medium examinations-consensus statements from Italian College of Radiology (SIRM), Italian College of Nephrology (SIN) and Italian Association of Medical Oncology (AIOM). Radiol Med 2022; 127: 534-542.
128) van der Lubbe MFJA, Vaidyanathan A, de Wit M, van den Burg EL, Postma AA, Bruintjes TD, Bilderbeek-Beckers MAL, Dammeijer PFM, Bossche SV, Van Rompaey V, Lambin P, van Hoof M, van de Berg R. A non-invasive, automated diagnosis of MeniÃ¨re's disease using radiomics and machine learning on conventional magnetic resonance imaging: A multicentric, case-controlled feasibility study. Radiol Med 2022; 127: 72-82.
129) Sardanelli F, Trimboli RM, Houssami N, Gilbert FJ, Helbich TH, Ãlvarez Benito M, Balleyguier C, Bazzocchi M, Bult P, Calabrese M, Camps Herrero J, Cartia F, Cassano E, Clauser P, Cozzi A, de Andrade DA, de Lima Docema MF, Depretto C, Dominelli V, Forrai G, Girometti R, Harms SE, Hilborne S, Ienzi R, Lobbes MBI, Losio C, Mann RM, Montemezzi S, Obdeijn IM, Ozcan UA, Pediconi F, Pinker K, Preibsch H, Raya Povedano JL, Sacchetto D, Scaperrotta GP, Schiaffino S, Schlooz M, SzabÃ³ BK, Taylor DB, Ulus Ã–S, Van Goethem M, Veltman J, Weigel S, Wenkel E, Zuiani C, Di Leo G. Magnetic resonance imaging before breast cancer surgery: results of an observational multicenter international prospective analysisÂ (MIPA). Eur Radiol 2022; 32: 1611-1623.
130) Petralia G, Zugni F, Summers PE, Colombo A, Pricolo P, Grazioli L, Colagrande S, Giovagnoni A, Padhani AR; Italian Working Group on Magnetic Resonance. Whole-body magnetic resonance imaging (WB-MRI) for cancer screening: recommendations for use. Radiol Med 2021; 126: 1434-1450.
131) Negroni D, CassarÃA, Trisoglio A, Soligo E, Berardo S, Carriero A, Stecco A. Learning curves in radiological reporting of whole-body MRI in plasma cell disease: a retrospective study. Radiol Med 2021; 126: 1451-1459.
132) Feraco P, Piccinini S, Gagliardo C. Imaging of inner ear malformations: a primer for radiologists. Radiol Med 2021; 126: 1282-1295.
133) Russo L, Gui B, Miccò M, Panico C, De Vincenzo R, Fanfani F, Scambia G, Manfredi R. The role of MRI in cervical cancer > 2 cm (FIGO stage IB2-IIA1) conservatively treated with neoadjuvant chemotherapy followed by conization: a pilot study. Radiol Med 2021; 126: 1055-1063.
134) Brizi MG, Perillo F, Cannone F, Tuzza L, Manfredi R. The role of imaging in acute pancreatitis. Radiol Med 2021; 126: 1017-1029.
135) Ricatti G, Veronese N, Gangai I, Paparella M, Testini V, Guglielmi G. Hoffa's fat pad thickness: a measurement method with sagittal MRI sequences. Radiol Med 2021; 126: 886-893.
136) Trombadori CML, D'Angelo A, Ferrara F, Santoro A, Belli P, Manfredi R. Radial Scar: a management dilemma. Radiol Med 2021; 126: 774-785.
137) Pontone G, Di Cesare E, Castelletti S, De Cobelli F, De Lazzari M, Esposito A, Focardi M, Di Renzi P, Indolfi C, Lanzillo C, Lovato L, Maestrini V, Mercuro G, Natale L, Mantini C, Polizzi A, Rabbat M, Secchi F, Secinaro A, Aquaro GD, Barison A, Francone M. Appropriate use criteria for cardiovascular magnetic resonance imaging (CMR): SIC-SIRM position paper part 1 (ischemic and congenital heart diseases, cardio-oncology, cardiac masses and heart transplant). Radiol Med 2021; 126: 365-379.
138) Neri E, Granata V, Montemezzi S, Belli P, Bernardi D, Brancato B, Caumo F, Calabrese M, Coppola F, Cossu E, Faggioni L, Frigerio A, Fusco R, Petrillo A, Girardi V, Iacconi C, Marini C, Marino MA, Martincich L, Nori J, Pediconi F, Saguatti G, Sansone M, Sardanelli F, Scaperrotta GP, Zuiani C, Ciaghi E, Montella M, Miele V, Grassi R. Structured reporting of x-ray mammography in the first diagnosis of breast cancer: a Delphi consensus proposal. Radiol Med 2022; 127: 471-483.
139) Granata V, Faggioni L, Grassi R, Fusco R, Reginelli A, Rega D, Maggialetti N, Buccicardi D, Frittoli B, Rengo M, Bortolotto C, Prost R, Lacasella GV, Montella M, Ciaghi E, Bellifemine F, De Muzio F, Grazzini G, De Filippo M, Cappabianca S, Laghi A, Grassi R, Brunese L, Neri E, Miele V, Coppola F. Structured reporting of computed tomography in the staging of colon cancer: a Delphi consensus proposal. Radiol Med 2022; 127: 21-29.
140) Fusco R, Setola SV, Raiano N, Granata V, Cerciello V, Pecori B, Petrillo A. Analysis of a monocentric computed tomography dosimetric database using a radiation dose index monitoring software: dose levels and alerts before and after the implementation of the adaptive statistical iterative reconstruction on CT images. Radiol Med 2022; 127: 733-742.
141) Sansone M, Marrone S, Di Salvio G, Belfiore MP, Gatta G, Fusco R, Vanore L, Zuiani C, Grassi F, Vietri MT, Granata V, Grassi R. Comparison between two packages for pectoral muscle removal on mammographic images. Radiol Med 2022; 127: 848-856.